Journal of the Korean Physical Society, Vol. 54, No. 4, April 2009, pp. 1475∼1480

# Field Mapping System for the KIRAMS-30 Cyclotron Magnet

K. H. Park,* Y. D. Yoon, Y. G. Jung, D. E. Kim and B. K. Kang
*Pohang Accelerator Laboratory and Department of Electrical Engineering, Pohang University of Science and Technology, Pohang 790-784*

J. Kang
*Cyclotron Application Laboratory, Korea Institute of Radiological and Medical Science, Seoul 139-706*

J. S. Chai
*School of Information & Communication Engineering, Sungkyunkwan University, Suwon 440-764*

(Received 12 August 2008, in final form 5 December 2008)

This paper presents a Hall-probe mapping system for measuring a cyclotron magnet. The system fabricated for the 30-MeV cyclotron at the Korea Institute of Radiological and Medical Sciences (KIRAMS). The Hall probes were mounted on a precision mechanical rotational stage and mapped the magnetic field in a cylindrical coordinate system. The mapping system used the "flying" mode field mapping method to reduce the data-acquisition time. The time required for mapping the whole gap-area of the cyclotron magnet was ∼75 minutes. The relative random fluctuation error during the entire mapping process was less than ±0.01 %. The cyclotron magnet was corrected using the measured data for the magnetic field. After the correction, the total phase excursion of the cyclotron was less than ±12°, which is within the total phase excursion tolerance of ±20°.

PACS numbers: 41.20.-q
Keywords: Cyclotron, Magnet field measurement, Hall-probe

## I. INTRODUCTION

The 30-MeV cyclotron at the Korea Institute of Radiological and Medical Sciences (KIRAMS-30) has been developed for producing radioisotopes, such as $^{18}$F and $^{123}$I, for positron emission tomography (PET) applications and for ion-beam experiments [1, 2]. The major machine parameters and the requirements of the magnetic field mapping system for KIRAMS-30 are listed in Table 1. The specified relative accuracy for the magnetic field measurement is ±0.01 %. Magnetic field mapping is necessary to correct and confirm the field quality of the manufactured magnet. This process requires iterated and tedious work: measuring the field and shimming the magnet pole, repeatedly.

The KIRAMS-13 cyclotron was developed successfully by the KIRAMS and was installed in five different locations in South Korea for PET experiments. The magnet shape of the KIRAMS-13 cyclotron was H-type so that the magnetic pole to be measured the field profile was easy to access from the outside. Thus the mapping system could be installed easily with a rectangular coordinate system by using a $x - y$ stage with stepping motors and ball screws with a simple measurement scheme [3]. However, the KIRAMS-30 cyclotron has a cylindrical-type magnet. The magnetic pole is enclosed by the circular return yoke, except for small holes for beam extraction and other purposes. The mapping stage should be installed in a small gap. All driving devices are attached below the bottom return yoke. All cables and mechanical forces are transferred only through the small holes. The Hall- probe carrier has to be moved in radial and azimuthal directions without any mechanical vibration. A linear motor was applied for radial movement with a complicated architecture. Thus, the magnet measurement system for the KIRAS-30 is more complicated than the one for KIRAMS-13 and has to use a different method.

The Teslameter and Hall probes have been used widely to measure cyclotron magnets and insertion devices, such as undulators, wigglers and solenoids, which require a highly accurate magnetic field measurement [4,5]. The Hall-probe mapping systems for the cyclotron magnet measurement at many laboratories uses polar coordinates [6]. However, it is very difficult to build a large wheel for the mapping stage at a moderate cost and a thin wheel deforms in time while a thick wheel tends to be too heavy to handle.

This paper presents a Hall-probe mapping system for

*E-mail: pkh@postech.ac.kr; Fax: +82-54-279-1399

Table 1. Major parameters of the KIRAMS-30 cyclotron and the specifications of the magnetic field mapping system.

| System specification | Unit | Value | System specification | Unit | Value |
|---|---|---|---|---|---|
| Maximum energy | MeV | 30 | Radio frequency | MHz | 63.96 |
| Number of sectors | | 4 | Hill angle | degree | 48 |
| Hill gap | mm | 30 | Beam current | $\mu$A | 500 |
| Range of magnetic field | T | 2 | Position accuracy | $\mu$m | <10 |
| Accuracy of measurement system | gauss | $\pm$2 | Mapping time | minute | $\sim$75 |
| Measurement resolution radial | mm | 10 | Measurement resolution angle | degree | 0.04 |
| Rotation angle | degree | $\pm$360 | Radial scan length | mm | 800 |

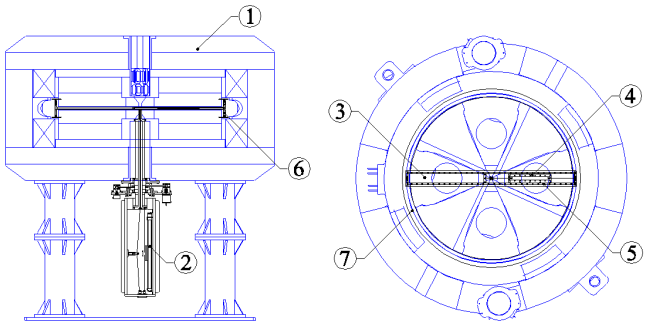


Fig. 1. Cross sectional views of the Hall probe mapping system and the KIRAMS-30 cyclotron magnet: ①: KIRAMS-30 cyclotron magnet, ②: driving stage, ③: mapping stage , ④: Hall-probe carrier, ⑤: guide frame, ⑥: roller module and ⑦: circular guide panels.

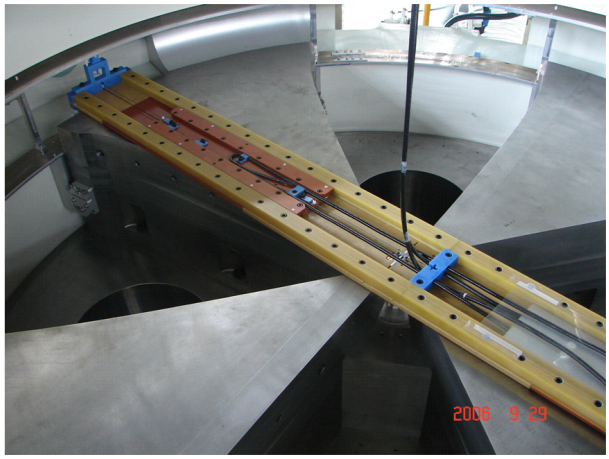


Fig. 2. Mapping stage installed in the pole gap. We can see the roller module, the Hall-probe carrier and the guide frame. The Hall-probe cables come down the hole at the upper return yoke.

the KIRAMS-30 cyclotron magnet and the results of the magnetic measurement. Two Hall probes were mounted on one Hall probe carrier, which was driven using two motors: one for circular motion and the other for radial motion. They mapped the magnetic field in cylindrical coordinates. To reduce the time for data acquisition, the system used the "flying" mode field-mapping method in which the data acquisition was done while the Hall probe moved [3]. The implemented mapping system took only 75 minutes to map the whole area of the pole with 800 thousand measurement points, which is much faster than the other one [7]. The details of the mechanical mapping stage and a brief description of the electrical measurement system are given in Section II, the results of the magnetic measurement are given in Section III and conclusions are given in Section IV.

## II. HALL PROBE MAPPING SYSTEM

### 1. Mechanical System

The magnet and the measurement systems were mounted on a steel plate and a rubber pad to absorb floor vibration and to compensate for uneven floor surface. Cross-sectional views of the Hall probe mapping system and the KIRAMS-30 cyclotron magnet ① are given in Figure 1. The Hall-probe mapping system consists of two stages: the driving stage ② and the mapping stage ③, as shown in Figure 1. The mapping stage consists of the Hall-probe carrier ④, a guide frame ⑤ and two roller modules ⑥, which are mounted at both ends of the guide frame. Three small wheels are attached to the roller module: one wheel at the top and the other two wheels at the bottom. Two circular guide panels ⑦ are installed between the magnetic coils to support the roller modules. By the help of the roller modules, the guide frame rotates continuously at the mid plane of the magnet pole gap without any friction or slow mechanical vibration.

The Hall-probe carrier is installed on the guide frame. As shown in Figure 2, the guide frame has two v-shaped grooves, which guide the Hall-probe carrier smoothly in the radial direction. Each side of the Hall-probe carrier has four small v-shaped wheels that fit in the v-grooves

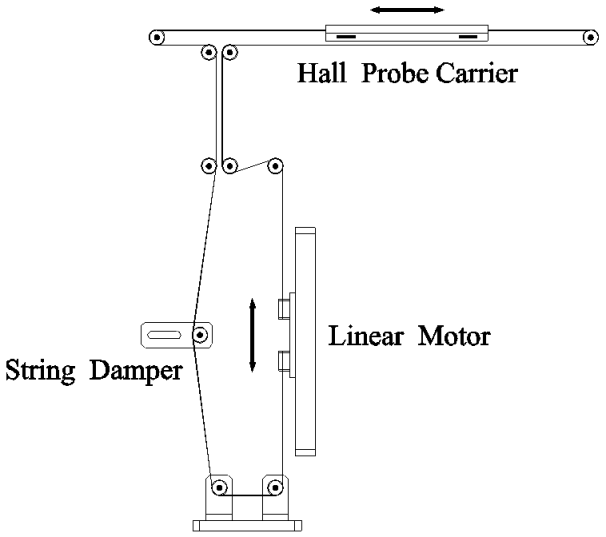


Fig. 3. Driving system of the Hall-probe carrier for the radial motion.

on the guide frame. Two Hall probes are placed on the longitudinal axis of the Hall-probe carrier. The separation between two Hall probes is 400 mm. The guide frame, the Hall-probe carrier and the roller modules are made of nonmagnetic epoxy fiber-glass, Bakelite and engineering plastic materials, respectively.

The driving system for the radial motion of the Hall-probe carrier is shown in Figure 3. A linear motor is attached to a string and pulley system that converts the up-down motion of the linear motor into a radial motion for the carrier. The string is a polyester monofilament line, Max Challenge 1.2, from Samchil Co. This thin nonmagnetic line, which can support very high tension, was chosen after several experiments with different materials. A mechanical damper adjusts the string tension.

### 2. Driving and Data acquisition System

A block diagram of the electrical system for field mapping is shown in Figure 4. It consists of two Teslameters, two digital voltmeters (DVMs), a stepping motor, a rotary encoder, a trigger pulse generator, a linear actuator and a data acquisition computer. The magnetic field was measured using two DTM-141 Teslameters and two MPT-141 Hall probes from Group3 Technology Ltd. The active area of the Hall probe is 1.0 mm × 0.5 mm. The output voltages of the Teslameters are digitized in two HP3458A DVMs from Agilent Technologie whenever a pulse from the trigger pulse generator triggers the DVM.

A stepping motor AX83-135, driver A-series and a controller OEM010 from Paker Co. were used to rotate the guide frame. The stepping motor was operated in the micro-step mode in 25000 steps / revolution to obtain a smoothing movement. The rotary encoder, S66-5-

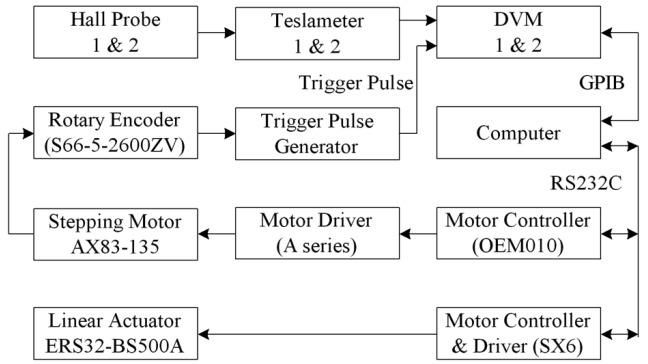


Fig. 4. Block diagram of the electrical system for field mapping.

3600ZV, from Metronics and a homemade trigger pulse generator outputs 9000 pulses / revolution. Accordingly, the output voltage of the Teslameter is digitized at every 0.4° rotation of the guide frame while the guide frame rotates continuously for the "flying" mode field measurement. The rotary encoder outputs one $z$-clock for every 360° revolution. The first $z$-clock was used as the starting point of the measurement. To reduce the measurement time, we measured the magnetic fields while rotating the guide frame in clockwise and counter-clockwise directions. The ERS32-BSS500A linear actuator and the SX6 stepping motor driver from Paker Co. provided the radial movement of the Hall-probe carrier. The stroke of a linear actuator was 500 mm, which is sufficient for the 400 mm distance.

## III. MEASUREMENT RESULTS

### 1. Hall-probe Calibration

A fast field mapping is required to reduce drift of the Hall-probe output signal due to temperature fluctuations. The measurement system uses two Hall probes and Teslameters to shorten the measurement time by one half. The responses of the Hall probes to changes in the magnetic field and in the ambient temperature are nonlinear and a built-in calibration table on PROM is provided for the MPT series Hall probes. Thus, we could use the built-in calibration table to compensate for the nonlinearities of Hall probes. However, the DTM-141 Teslameter has no option for sampling the field by using an external trigger signal. A data sampling at an exact time is very important for the "flying" mode field measurement for which the probe does not stop for the measurement. Because of these reasons, we did not use the built-in calibration table. Instead, an off-line calibration table for the Hall probe was constructed and it was used to calibrate the measured data.

For the "flying" mode field measurement, the analog output voltage of the Teslameter was digitized using the

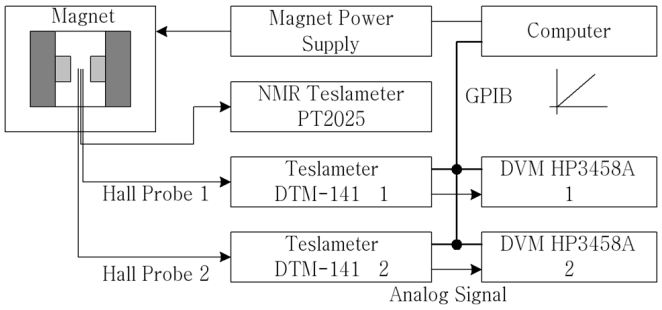


Fig. 5. Block diagram for the Hall probe calibration.

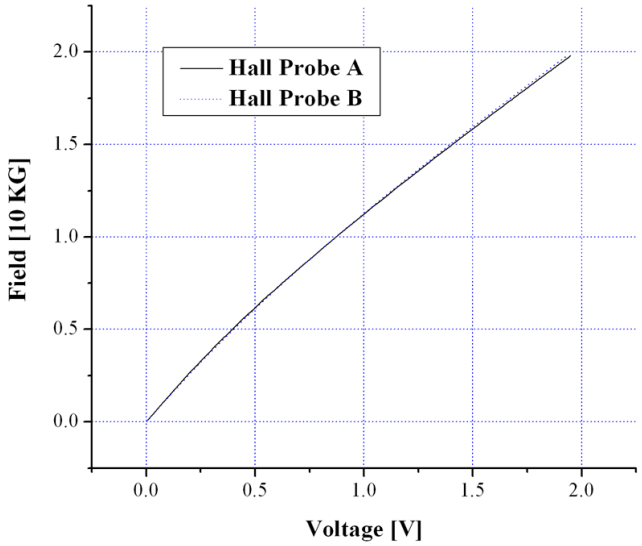


Fig. 6. Constructed calibration table.

HP3458A DVM, which has an external trigger clock input. Block diagrams for the Hall-probe calibration system and the constructed calibration table are shown in Figures 5 and 6, respectively. To construct the calibration table, we used the PT2025 NMR Teslameter from Metrolab and found two pairs of Teslameters and Hall probes that showed similar field readings. Then, the calibration table shown in Figure 6 was obtained by logging the Teslameter readings and the analog output voltage of the Teslameter while increasing the magnet current.

## 2. Field Measurement

The voltages measured using the DVMs were converted into magnetic fields by using the off-line calibration table and were interpolated using the cubic spline method. To measure the noise level of the measurement system, we put the Hall probes into zero-gauss chambers to shield the terrestrial magnetic field and they were mapped on the mapping stage. The system noise data were sampled every 0.4° and the results are shown in Figure 7. The measured system noise is about ±2.0 Gauss,

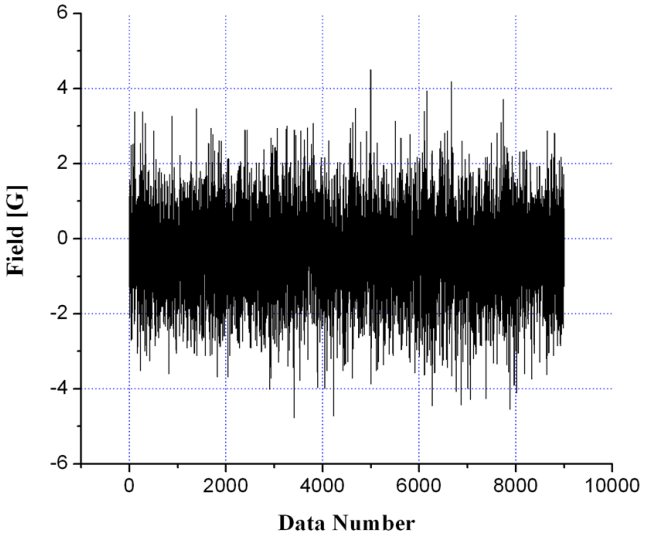


Fig. 7. Measured system noise in units of Gauss.

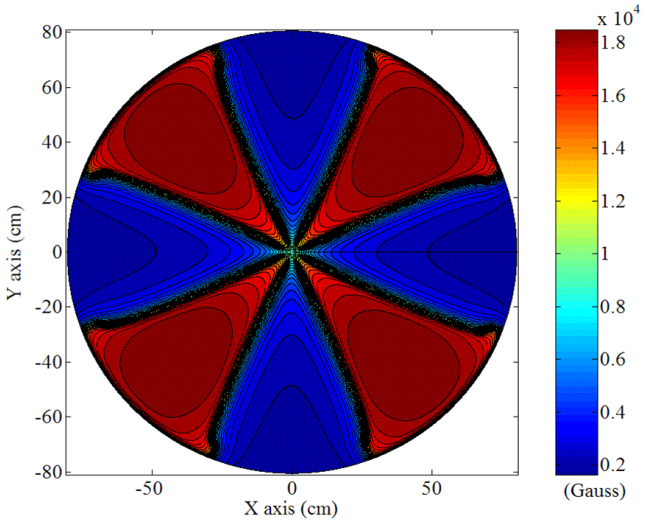


Fig. 8. Measured field profile of the KIRAMS-30 cyclotron magnet.

which satisfies the specified accuracy of field measurement given in Table 1.

The results of Hall-probe mapping for the KIRAMS-30 cyclotron magnet at an excitation current of 134 A is shown in Figure 8. This figure shows a typical profile of a magnetic field for a cyclotron magnet. The measured magnetic fields at the hill and the valley are ∼1.9 T and ∼0.2 T, respectively.

The magnetic field profile of the initial magnet was significantly different from the designed one, for various reasons, such as differences in magnet material, fabrication error, *etc.* The measured magnetic field data were used to correct the magnet. The correction was made on the sidewalls of the magnet by adding or removing iron shims and it was repeated until the magnetic field profile was close to the designed one. The model and the mea-

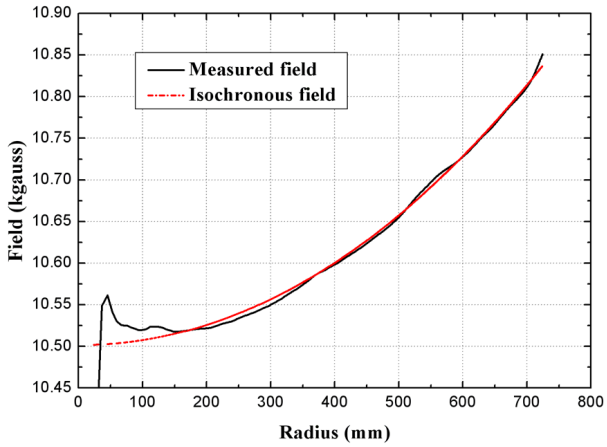


Fig. 9. Average magnetic field along the isochronous field as a function of the average radius.

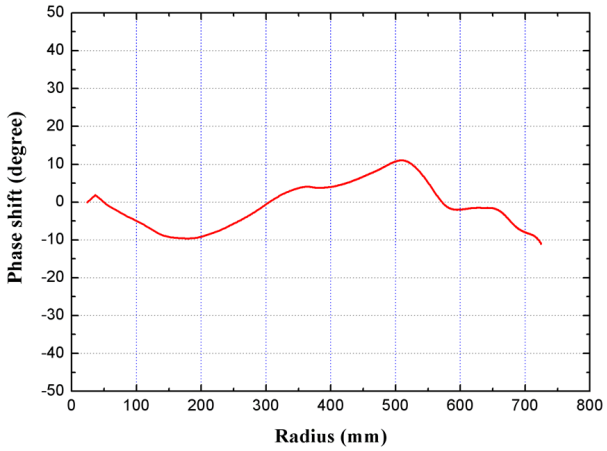


Fig. 10. Phase excursion of a particle versus average radius.

sured average magnetic field along the isochronous field are shown in Figure 9. The difference between the designed and the measured fields is ∼0.1 %, which can be compensated for easily by adjusting the RF frequency. The RF amplifier of the KIRAMS-30 cyclotron has the 63.96 MHz of the center frequency and its tuning range is ±1.5 MHz [8]. The field difference of 0.1 % corresponds to ∼60 kHz, which is much smaller than the amplifier's tuning range.

The average magnetic field shown in Figure 9 increases slowly along the radius in accordance with the isochronous requirement given as

$$\omega = \frac{q < B(r) >}{\gamma(r) m_0}, \tag{1}$$

where $\omega$ is the angular frequency of a particle, $< B >$ is the average magnetic field, $q$ is the charge of the particle, $\gamma$ is the usual relativistic factor and $m_0$ is the rest mess of the particle. The relativistic factor $\gamma$ increases with the radius $r$. Thus, to satisfy the Eq. (1) when the RF driving frequency is fixed, the average magnetic field $< B >$ should also increase with radius $r$ to compensate for the relativistic mass gain of the accelerated particle. Because there is no sector structure in the central region, a magnetic field of less than 100 mm in radius has been raised. A decreasing magnetic field with radius is required to focus the beam about the central region.

Deviations from an isochronous field result in a phase slip of the particle, which is usually expressed as

$$\sin\phi(E) = \sin\phi_0 = 2\pi h/qV \int_{E_i}^{E} (\omega_{rf}/\omega(E) - 1) dE, \tag{2}$$

where $\phi(E)$ is the phase excursion at energy $E$, $\phi_0$ is the initial phase, $h$ is the harmonic number, $V$ is the dee voltage, $\omega_{rf}$ is the angular RF frequency and $\omega(E)$ is the angular frequency of the particle at energy $E$ [9].

The acceleration angle by the RF dees of the KIRAMS-30 cyclotron is 39°, which was given by the design parameter. The allowable phase error of the KIRAMS-30 cyclotron is limited to ±19.5° to accelerate the beam securely. If the phase error was to be increased, the beam loss would also be increased. The total phase excursions versus average radius for the measured field are shown in Figure 10. These results indicate that the total phase excursion after correction is less than ±12°, which is acceptable for the KIRAMS-30. Further details on the magnetic measurement and the analysis are described in Ref. 8. The KIRAMS-30 cyclotron was installed at the Advanced Radiation Technology Institute in Jungup city in 2007 and it is operating well at a beam current of 500 $\mu$A.

## IV. CONCLUSION

A Hall-probe mapping system has been developed for measuring the KIRAMS-30 cyclotron magnet. It uses the "flying" mode field mapping method to reduce the data-acquisition time and maps the magnetic field in cylindrical coordinates. The time required for mapping the whole gap-area of the cyclotron magnet is ∼75 minutes and the field data are sampled at a step of 0.4° in the circular-direction and 10 mm in the radial-direction. The relative random fluctuation error during the entire mapping process is less than ±0.01 %. The cyclotron magnet has been corrected using the field measurement data and the total phase excursion of the cyclotron achieved after correction is less than ±12°.

## ACKNOWLEDGMENTS

This work was supported by the Ministry of Education, Science and Technology.

## REFERENCES


[1] J. Kang, B. H. Hong, D. H. An, H. S. Chang, I. S. Hung, J. S. Chai, M. G. Hur, T. K. Yang and Y. S. Kim, *Design Study of the 30-MeV Cyclotron Magnet* (EPAC 06, Edinburgh, 2006), p. 2559.

[2] J. Kim, J. Korean Phys. Soc. **52**, 738 (2008).

[3] K. H. Park, Y. G. Jung, D. E. Kim, B. K. Kang, M. Yoon, J. S. Chai and Y. S. Kim, NIM A **545**, 533 (2005).

[4] S. Marks, IEEE Ttrans. on Magnet **30**, 2435 (1984).

[5] K. H. Park, Y. G. Jung, D. E. Kim, H. G. Lee, S. J. Park, B. K. Kang and C. H. Chung, J. Korean Phys. Soc. **50**, 950 (2007).

[6] M. Fan, X. Zhang, T. Zhang, C. Liang, Q. Tao, Z. Chao, C. Chu, T. Li, Y. Hu, Y. Chen, H. Zhang, H. Jia, C. Jiao, J. Liu, W. Zhang, C. Zhou, J. Jiao and Y. Hou, *Measurement and Adjustment of CIAE Medical Cyclotron magnet* (PAC 1993, Washington D.C., 1993), p. 2841.

[7] A. Geisler, C. Baumgarten, A. Hobl, U. Klein, D. Krischel, M. Shillo and J. Timmer, *Status report of the ACCEL 250-MeV Medical Cyclotron* (Cyclotron Conference, Tokyo, 2004).

[8] I. S. Jung, D. H. An, B. H. Hong, J. S. Kang, M. G. Hur, H. S. Jang, T. G. Yang, M. Y. Lee, S. S. Hong, Y. S. Kim and J. S. Chai, *Design of the RF System for 30-MeV Cyclotron* (EPAC 06, Edinburgh, 2006), p. 1340.

[9] S. H. Shin, M. Yoon, E. S. Kim, K. H. Park and J. S. Chai, J. Korean Phys. Soc. **45**, 1045 (2004).